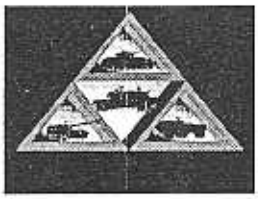

TARDEC

NVESD

KRC
Keweenaw Research Center

Volume I
Proceedings
Sixth Annual

Ground Target Modeling and Validation Conference

August 1995

at
Michigan Technological University
Houghton, Michigan

The simulation of an IR FPA sensor

Gideon Baum, Yossi Bushlin
EORD, Technion R&D foundation LTD, Haifa, Israel
EMAIL: qars003@vmsa.technion.ac.il

Doron Cohen
IDF - Israel Defense Forces

ABSTRACT

The intensive development and use of IR FPA imaging systems has raised the need for a reliable simulation tool to be used for operation research of new technologies and training of system users.

This paper presents our FPA model. The model is based on measurable characteristic parameters of the FPA sensor and takes into consideration the detector response, fixed pattern noise and temporal noise.

The model was implemented into a software code written in C (running on a SGI Indigo workstation) with emphasis on a modular program structure and on a mouse event driven graphic user interface. The input to the software is similar to that of the TTIM (TACOM Thermal Image Model) code and includes a high resolution radiometric map and a set of sensor parameters. The Optics transfer functions are implemented by a convolution, thus allowing a more general treatment. The FPA detector model includes accurate spatial sampling (including pitch) and 12-bit digitization of the signal. A set of signal and image processing functions were prepared, allowing the user to simulate algorithms implemented on existing systems or to test new algorithms.

The simulated image is displayed on a graphic window with the temporal noise animated at real-time. Display parameters like contrast, brightness, zoom and system parameters such as the gain and level are controllable from the GUI (Graphic User Interface). The graphic window is transferred also to a video output by the SGI Galileo card thus generating a standard video image.

INTRODUCTION

The use of simulation tools for generating images (and video clips) of scenarios where a thermal sensor observes a given scene is becoming more and more extensive. The simulation is used for various purposes such as training, design of new sensors, creating data bases for ATR algorithms and more. For a realistic simulation of various combat scenarios, there is a need for a reliable and easy to use sensor model.

In a previous work [1] the results of a validation test for the TTIM sensor model [2] were described. It was found that there are two different types of errors concerned with the sensor model: Inherent errors caused by un modeled effects and parameter characterization errors. Based on the validation test results, the following guide lines for an improved sensor model were outlined: (*1*) The model should be based only on measurable characteristics of the sensors, (*2*) The model should enable the simulation of dynamic effects such as temporal noise and movements of the line of sight (LOS), (*3*) There is no use to model effects which will be altered or corrected by the electronics - only the overall result should be considered, (*4*) It should be possible to determine each detector element characteristic (sensitivity and noise) separately, (*5*) The software to be written should be modular and in a structure that will enable convenient maintenance of the code and easy upgrading.

According to these guide lines, a new sensor model is being developed at EORD for the simulation of thermal imagers. The emphasis of this paper is on the FPA (Focal Plane Array) sensor model. The structure of the software code is described in Fig. 1. The description for each module is included in the following section. Some preliminary results and comparison of calculated and measured images are included as well.

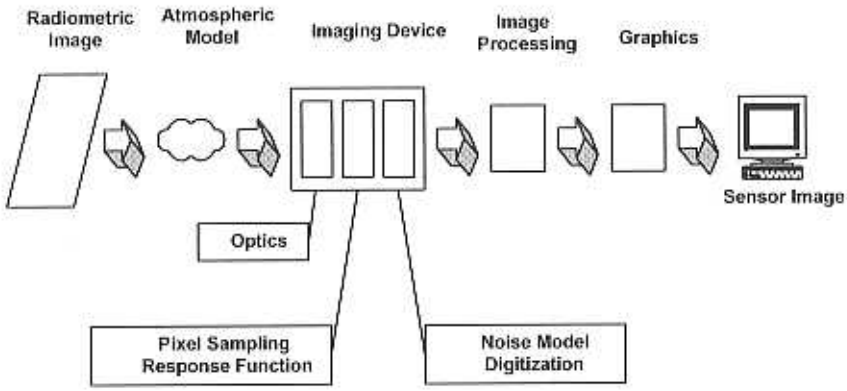

Figure 1 The modular structure of the simulation.

THE SIMULATION MODULES

This section will describe the theoretical models and their implementation into the various modules of the software.

Input

The input to the simulation software consists of two ASCII files, one contains the parameters characterizing the sensor and the other is the radiometric scene map.

The radiometric input data characterize the scene composed of the background and the targets as measured by a calibrated radiometer. The data is read from an ASCII file with a similar structure to the TTIM input file, consists of an header describing the radiometer data and the radiometric map. The radiometric units are either *Band Radiant Emittance:* [W] = Watt/(cm^2·str) or *Band Radiant Photon Emittance:* [Q] = #ph/(sec·cm^2·str) or *Temperature:* [T]=Kelvin.
The radiance units are converted according to the Planck distribution to radiant emittance at the sensor's bandwidth. Note that conversions from very different spectral bands as in the case of converting radiometric data measured in the 8-12 spectral band to the 3-5 μm band, do not consider variations due to spectral dependent effects such as emissivity and sun reflections.

Atmospheric Model

In the 1-5μm spectral band, where currently most of the FPA sensors are operating, the atmospheric transmittance and the Planck distribution are spectrally dependent quantities. Thus the weighted average Transmittance $\langle \tau_{atm} \rangle$ and the Path Radiance $\langle Q_{path} \rangle$ are calculated by:

$$\langle Q_{path} \rangle = \int_{\lambda_{min}}^{\lambda_{max}} Q_{path}(\lambda)\, d\lambda$$

$$\langle \tau_{atm} \rangle = \frac{\int_{\lambda_{min}}^{\lambda_{max}} \tau(\lambda)\, Q(\lambda, T_{scene})\, d\lambda}{\int_{\lambda_{min}}^{\lambda_{max}} Q(\lambda, T_{scene})\, d\lambda} \qquad (1)$$

The spectrally dependent atmospheric *Transmittance* $\tau(\lambda)$ and the *Path Radiance* $Q_{path}(\lambda)$ are calculated by the LOWTRAN-7 FORTRAN code. The atmospheric effect is implemented in the radiation map by the linear transformation $Q_i = \langle \tau_{atm} \rangle\, Q(T_i) + \langle Q_{path} \rangle$.

Optics

Two main optical effects were modeled in the simulation so far: *Optical Blurring* and *Diffraction*. Their MTF is written in the following equations (see also at [2,3]):

$$H_{blur}(k) = e^{-\pi^2 \omega_B^2 k} \tag{2}$$

$$H_{diff}(k) = \frac{2}{\pi}\left(\cos^{-1}(A) - A\sqrt{1-A^2}\right) \tag{3}$$

where: $A = \lambda_D \cdot f_\# \cdot k / F$; $k = \sqrt{k_x^2 + k_y^2}$ spatial frequency [cycle / mrad] ; λ_D = diffraction wavelength [micron] ; $f_\#$ = optical F - number ; $\omega_B = e^{-1}$ half - width optical PSF [mrad] ; F = optical focal length [mm].

The $OTF = H_{Diff} \cdot H_{blur}$ is calculated with the user supplied optical parameters. Alternatively the user may supply a measured OTF table. By calculating the Fourier transform of the OTF, the PSF is obtained. The kernel representing the PSF is extracted by integrating it over intervals of the size of the radiometric IFOV. The optical effect is implemented on the radiometric map by convolution with the kernel. The advantage of using a convolution technique rather than FFT is the flexibility achieved and the possibility to consider non-isoplanar optical blurring effects.

Spatial Sampling

The FPA detector is modeled by a matrix of $N_x * N_y$ elements, separated by non active areas. The radiance Q_i on each detector element is sampled from the given radiometric map accounting for the radiometer and sensor IFOV's and ranges to the target, and the sensor's Pitch . The sampling model is an exact geometrical description (see figure 2) of a FPA. It is also applicable for a system with *microscan* sampling.

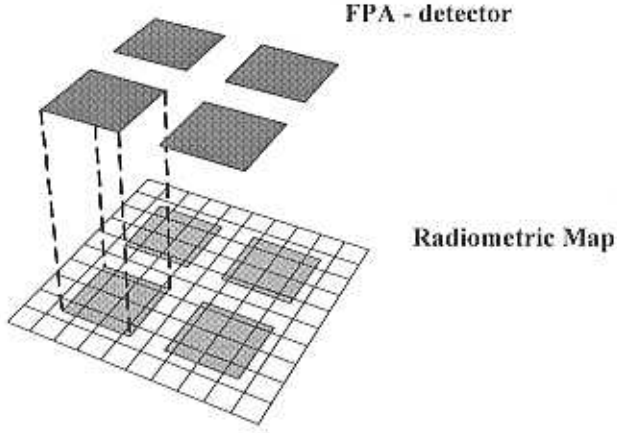

Figure 2 Spatial Sampling.

Detector Response

For uniform illumination by e.g. an extended blackbody, in the absence of optics and disregarding dark currents, the output voltage from the FPA is related to the radiance according to the formula [3]:

$$V = \frac{1}{N_{\max}} t_{int} \eta_{det} A_{det} \frac{1/\eta_{CS}}{4(f_\#)^2} Q(T) = \frac{Q(T)}{Q_{\max}} \tag{4}$$

where: η_{CS} = cold shield efficiency; A_{det}= sensitive area of each pixel; η_{det} = Quantum efficiency; t_{int} = FPA integration time; N_{max} = well capacity [# electrons] and V is the normalized voltage (V=1 for saturation). For convenience we define a quantity Q_{max} for which V=1. Note that a uniform spectral response was assumed.

By using eq. (4) and considering the optics and offset voltage, the relation of the nominal signal in the output of the i'th FPA pixel to the incoming radiation is given by:

$$V_i = V_0 + \eta_{CS}\tau_{opt}\frac{Q_i}{Q_{\max}} \tag{5}$$

where: V_0 = offset voltage (see expression below) ; Q_i = scene radiance map at the i'th pixel τ_{opt} = average transmission of the optics.

The offset voltage originates from the integration of dark current, radiance from inner parts of the sensor, self-emission of the optics, and internal reflections:

$$V_0 = \frac{1}{N_{\max}} t_{\text{int}} \frac{I_d}{q} + (1-\eta_{CS})\frac{Q(T_{opt})}{Q_{\max}} + \eta_{CS}\varepsilon_{opt}\frac{Q(T_{opt})}{Q_{\max}} \tag{6}$$

where: I_d = dark current [Amper]; q = charge of electron [Cb] ; $Q(T_{opt})$ = radiance from inner parts of the sensor; ε_{opt} = effective emisivity of the optics.

The notation "effective" emmisivity is used since the optics emmision is treated as if it was originating from the aperture. This effective emmision should include also the contribution of internal reflections. For the "worst case" estimation, one may use $\varepsilon_{opt} \approx 1-\tau_{opt}$.

Eq. (5) refers to the nominal (normalized) voltage in the output of the FPA. The actual voltage should include both temporal (ν_i) and fixed pattern non-uniformity noise (δ_i), namely:

$$V_i' = V_i + \delta_i + \nu_i \tag{7}$$

Temporal Noise

The *rms* of the temporal noise at each pixel, conventionally expressed in units of [#electrons], may be computed by $\sqrt{N_{floor}^2 + N}$ where the first term under the square root is the constant noise floor, and the second term is the shot noise $\sqrt{N}$ squared. "N" by itself represent the signal V_i in units of [#electrons]. Converting to normalized units, this formula for the *rms* of the temporal noise takes the form:

$$\sqrt{\langle \nu_i^2 \rangle} = \frac{1}{\sqrt{\kappa}} \cdot \sqrt{\left(\frac{N_{floor}}{N_{\max}}\right)^2 + \frac{V_i}{N_{\max}}} \tag{8}$$

where: κ = averaging factor.

Measurements done on a commercial FPA have indeed proven that the *rms* of the temporal noise may be computed by eq. (8) (with κ=1). Moreover, from those measurements, both Nmax and Nfloor were determined without the need to rely on the specifications supplied by the producer.

In some FPA systems the frame generation rate is much higher than the video display rate. This enables the improvement of the signal to noise ratio by averaging successive frames. Therefore, the factor κ was added to eq (8) where its value should be the number of averaged frames. The parameter κ may be used also for the simulation of static pictures taking into account the human observer integration time. For example, assuming that the human eye integrates over 0.1sec and the frame rate is 30 Hz , the averaging factor κ should be set equal to 3.

The animation of the temporal noise is implemented by creating a buffer containing N Images (N~20) and displaying them in a random order. In each image for every pixel, a random value is generated according to a normal distribution with a *rms* calculated by eq. (8). This value is added to the pixel response V_i (see eq. (7)).

Fixed Pattern Noise

In all conventional staring sensors the raw non-uniformities are treated by the electronics, therefore the simulation should consider only the **residual** non-uniformity which may be characterized by the so called "W-curve" defined by :

$$\mu(V)=\frac{\sqrt{\langle \delta_i^2(V)\rangle}}{V} \tag{9}$$

$\mu(V)$ may be measured when the detector is uniformly illuminated by an extended blackbody and the frames are temporally averaged. The mean output voltage is V, and the ratio rms/mean as defined above (9) is the residual non-uniformity conventionally expressed in percentage. An example for **measured** W-curve is presented in figure 4.

For the simulation of a "static" picture (no LOS movement) it is trivial to generate the non-uniformity noise. One has to generate (for each pixel) a random number δ_i that is taken out from a normal distribution that has the *rms* of $V_i \cdot \mu(V_i)$ and zero average. However, for simulating a LOS movement, a more sophisticated approach is needed, since the whole response curve of each pixel should be determined in advance. It is assumed that the deviation of the response curve from linearity may be approximated by a 2nd order polynomial (see figure 3), and parametrized in the form:

$$\delta_i(V) = \alpha_i(V-A_i)(V-B_i) \tag{10}$$

$$V_i = V+\delta_i(V)$$

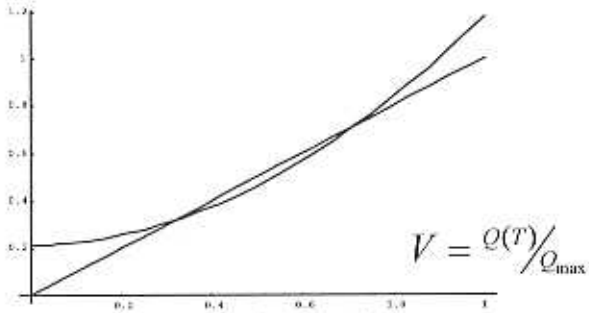

Figure 3 Non-Linearity of a pixel.

By averaging α_i, A_i, and B_i over all the pixels, assuming that these parameters are uncorrelated and $\langle\delta_i\rangle=0$ (for any V) and substituting eq. 10 into eq. 9, eq. 11 is obtained:

$$V\cdot\mu(V)=\langle\alpha^2\rangle\cdot\left(V^2-2\langle A\rangle V+\langle A^2\rangle\right)\left(V^2-2\langle B\rangle V+\langle B^2\rangle\right) \tag{11}$$

which is a quite general polynomial of the 4th degree. A best fit of eq. 11 to measured data is illustrated in figure 4 where a satisfactory match is achieved.

Hence a general scheme may be defined for generating the response curve of each pixel in the matrix once $\mu(V)$ is given. First, a 4th order polynomial best fit of the function $V\cdot\mu(V)$ from eq. (11) to the measured W-curve $\mu(V)$ is calculated, resulting in the determination of the averages and the standard deviations of the parameters α, A, and B. Then, the random values α_i, A_i, B_i for all the pixels in the matrix are generated from normal distributions with the previously determined statistics (the average and *std* of α, A, and B).

The resultant response curves, once generated, may be used in real-time simulation when LOS movement is expected. This model may be further developed to include spatial correlation of the residual fixed pattern noise.

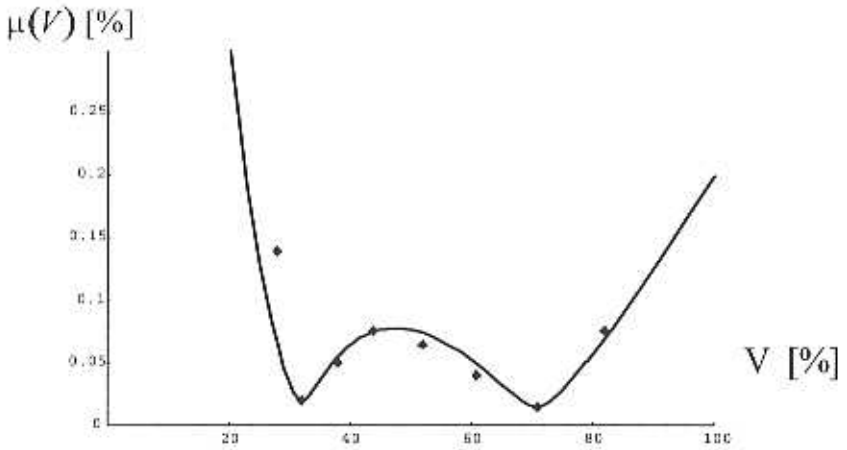

Figure 4 Measured μ(V) curve of the relative residual fixed pattern noise as function of the detector voltage. - Dots represent experimental results and the calculated fit of eq. (11) is given by the solid line. Note the characteristic *W* shape for a system with two points correction.

Digitization

The signal in the output of the FPA V_i' is pre-amplified and digitized for further processing. Thus, one should convert the (normalized) voltage to digital units.

$$V_i^{dgit} = \begin{cases} V_{\min} & V < V_{\min} \\ \text{int}\left(2^{\#bits} \dfrac{V_i' - V_{\min}}{V_{\max} - V_{\min}} \right) & other \\ V_{\max} & V > V_{\max} \end{cases} \tag{12}$$

The Range of the digitization ($V_{\min}$, $V_{\max}$) is controllable by the user. $V_{\min}$ is the voltage that corresponds to the least significant bit, while $V_{\max}$ corresponds to the most significant bit. Pixels at values outside the range ($V_{\min}$, $V_{\max}$) will be saturated.

Image Processing

In some sensors, image processing (I.P.) algorithms are implemented. The I.P. module may represent all kinds of image processing algorithms such as line duplication, histogram equalization, AGC, boost, etc. Therefor a generic interface to the I.P. function has been constructed in order to enable an easy implementation and replacement (at source level) of different algorithms. The I/O to the I.P. function is a structure containing all image data and parameters like number of pixels and gray levels. The I.P. function may create an output image of different size (as in the case of line duplication and zooming) or different number of grayscales (in AGC algorithms). In any case, memory allocation for the output image is made outside the I.P. function. The I.P. algorithm may simulate some nonlinear transformation of the 12-bits digitized signal to the analog converted 8-bits output video signal. However, in most available sensors the transformation is actually linear.

Graphical User Interface (GUI)

Up to this stage of the simulation development, the GUI includes only those controls that are related to the display of the sensor image - see Figure 5. A comprehensive GUI including all sensor and radiometric data is planned to be developed in the future.

The GUI gives the user control on the digitization range: ($V_{\min}$, $V_{\max}$). The updated values of $V_{\min}$,$V_{\max}$ are displayed and so is the histogram of the radiometric image at the detector plane. This tool enables the user to change interactively the dynamic range of the sensor and to observe how it is related to the range of radiation values getting into the sensor, and to see immediately it's influence on the obtained image.

Temporal noise may be switched On/Off by the "Temp Noise" button. Zoom, contrast and brightness of the sensor image are controllable (see Figure 5). An indication of the relation between the radiometric map and the sensor resolution is displayed, where at least a factor of 3 should be used [2]. The user may save to a file (in SGI format) the radiometric input or the sensor's calculated image. By using the four arrows, the user may simulate small 2D displacement of the sensor's LOS, which emphasize sampling effects and the influence of the fixed pattern noise .

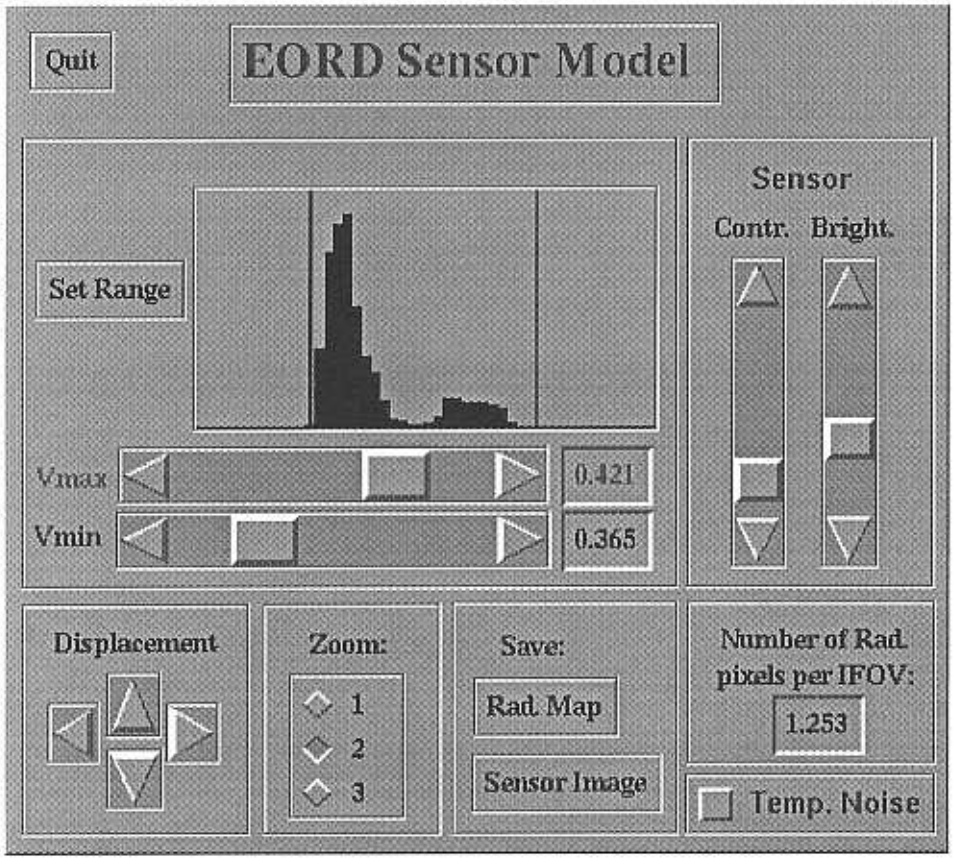

Figure 5 The GUI of the simulation.

The calculated image is displayed on the screen in a window of the size of the RS-170 video standard. In this window, pixels of the FPA which has no radiometric input are painted in gray. Pixels of the window for which there is no corresponding FPA pixel will remain black. The displayed window may be converted into standard RS-170 video by using the Galileo board and displayed on any video monitor.

The radiometric image is displayed as well on the computer monitor, where a rectangle representing the sensor FOV is outlined on the image (in the case that the sensor FOV is smaller than the radiometric map). This FOV indicator is updated when the user change the sensor's LOS.

DEMONSTRATION

The software was used for paramteric study of FPA sensors. A variety of images were generated for different sensor conditions. Some examples are enclosed. The basic sensor parameters that were used are listed in Table 1. These parameters are for a PtSi FPA.

The influence of number of pixels in the FPA detector and the influence of microscan technique is demonstrated in Figure 6. The simulation is of three trucks and a small power generator, placed in a desert background at day time at a range of 12.5 [km]. It is clearly seen how the obtained resolution is improved when applying the microscan.

TABLE 1 The Sensor parameters

Parameter	Value	Unit
Number of pixels (x,y)	320 244	
Pixel (width, height) IFOVX,IFOVY	22. 22.	μm
Pitch (width, height)	24. 24.	μm
Focal Length	200	mm
Bandpass of Detector (low, high)	3.4 4.1	μm
F# of optics	1.85	
Half-width of the optical system PSF	0.5	mrad
Transmission of Optics	0.65	
Effective emisivity of the optics	0.05	
Max capacity	1.E6	#electrons
Noise floor	150.	#electrons
Integration time	33.0	msec
Quantum efficiency of Detector	0.01	
Efficiency of Cold Shield	0.7	
Number of bits for sampling	12	

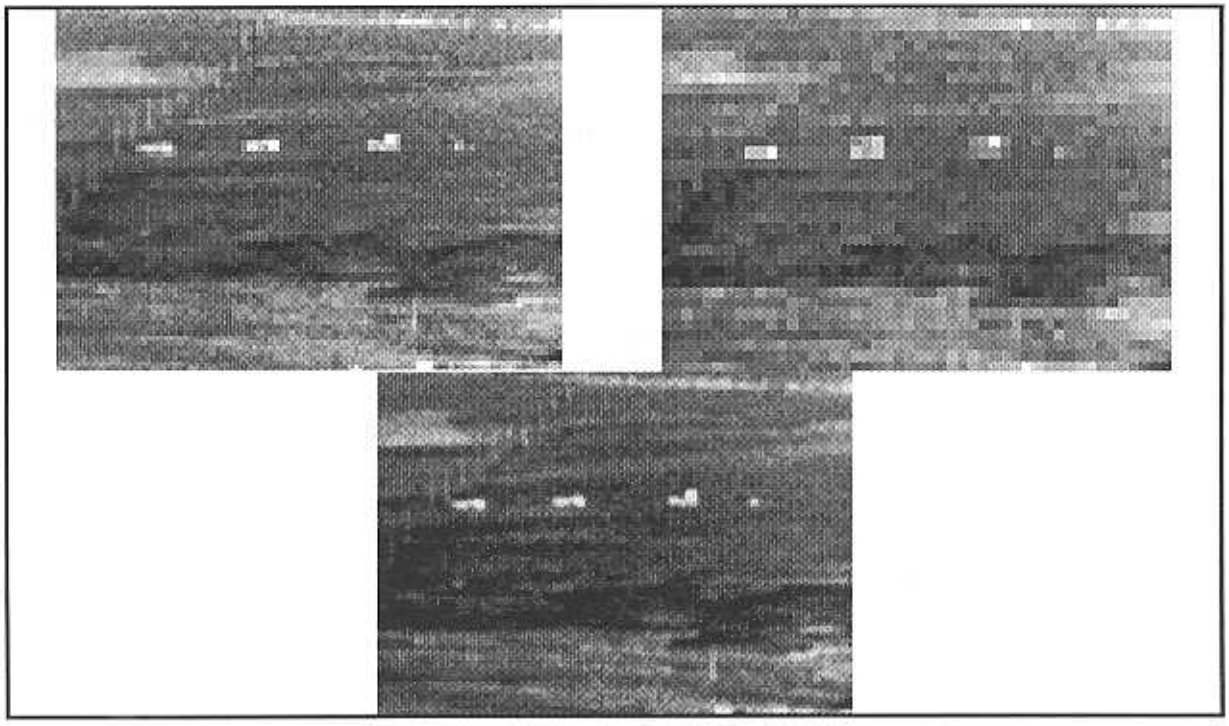

Figure 6 Simulated sensor image at 12.5 km, day time, with different matrix sizes. Upper left: the original number of pixels (see Table 1). Upper right: Half the number of pixels and double the pixel and pitch size. Lower: Original FPA with microscan.

The influence of the sensor integration time on the obtained image is demonstrated in figure 7. Note that as the integration time increases, the noise level decrease, and the hot parts of the scene are saturated. The saturation of the targets do not change their detectability but since all the target's details were lost, their recognition becomes impossible.

Any sensor model and simulation tool should be validated. The validation should include comparison between calculated and measured images [1], where the comparison should be done by human observers and by extracting quantitative

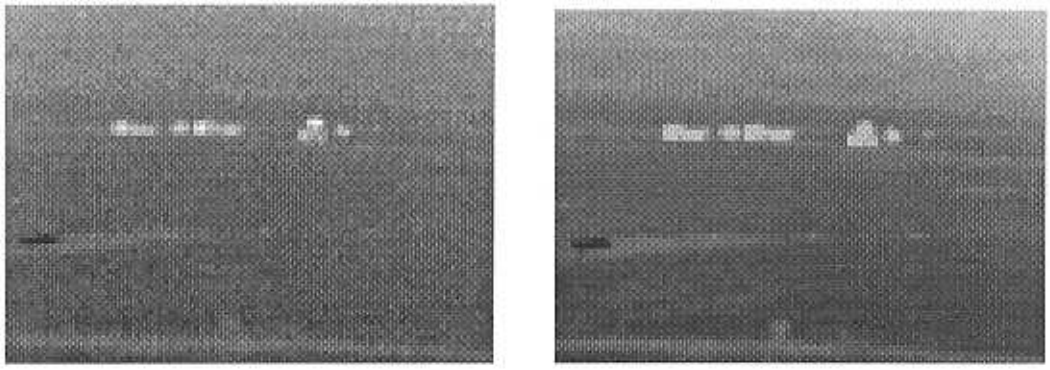

Figure 7 Simulated thermal FPA images of trucks. Left: the time integration was 33 [msec], Right: the time integration was increased by a factor of 10.

features from the images. At this stage we are at the beginning of the validation activity. An example for a preliminary result may be found in Figure 8 where two images are presented - calculated and measured with a good compatibility between them. The input to the simulation was a radiometric map of the van measured by an Inframetrics 760 radiometer operating in the 8-12μm band with a X-30 lens. The FPA sensor measured the same scene at the same time.

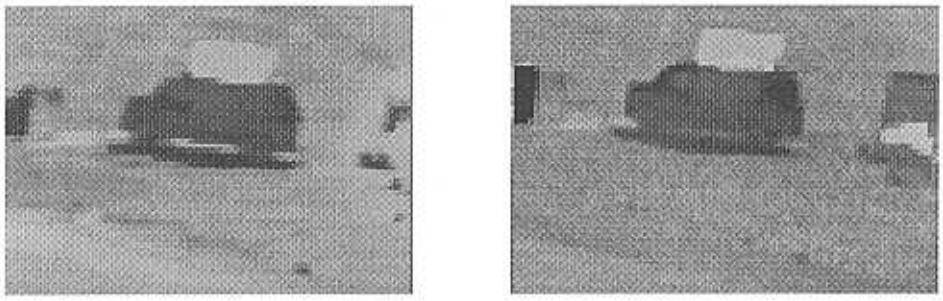

Figure 8 Measured (left) and simulated (right) images of a van with a hot plate on top at 1.1 km, day time.

CONCLUSION

A Sensor model for the simulation of a FPA thermal system was developed and presented. The model is based on measurable characteristic parameters of a real system. The software code implementing the model is capable of simulating dynamic effects such as temporal noise and LOS movements. Special consideration was paid to model the residual fixed pattern noise.

The work will be continued to improve the model and to include more new features into it (such as spatial correlation of the fixed pattern noise and more signal and image processing effects). Also the effort for validating the model under various conditions (complexity of the scene, time of day, various types of sensors, etc.) will be continued.

REFERENCES

1. Engel M., Bushlin Y., "Field Test Validation of the TTIM Sensor Model: Results and Comparison with a Real Sensor", Proceedings of the "Target Modeling and Validation Conference", KRC 1993

2. Hall C. S., Buxton E. T., Royne T. J. , "TACOM Thermal Image Model ver. 3.1 - Technical Reference and User's Guide", OptiMetrics,Inc. 1986.

3. Hudson R. D. ,"Infrared System Engineering", John Wiley & Sons, 1969.